22.4 A Reconfigurable Bidirectional Wireless Power Transceiver with Maximum-Current Charging Mode and 58.6% Battery-to-Battery Efficiency

Mo Huang[1,a], Yan Lu[1], Seng-Pan U[1,2], Rui P. Martins[1,3]

[1]University of Macau, Macau, China
[2]Synopsys Macau, Macau, China
[3]Instituto Superior Tecnico, Universidade de Lisboa, Portugal
[a]now with South China University of Technology, Guangzhou, China

Wireless power transfer (WPT) is currently on the critical point of an explosive growth. Here, as projected in Fig. 22.4.1, we propose a future WPT eco-system of consumer electronics, which includes three layers: 1) wireless charging pads being the fundamental energy plants that can charge a wireless power bank and mobile devices; 2) wireless power banks that get energy from plants and feed mobile devices; and 3) power hungry mobile devices that get energy from all the other sources. To enable the mobile devices charging others without additional hardware, we propose a reconfigurable bidirectional 6.78MHz WPT transceiver (TRX) that reuses the LC resonant tank and 4 area-consuming power transistors for the differential Class-D power amplifier (PA) and the full-wave rectifier. With such WPT TRX embedded, one can provide a first-aid to his/her smart watch or friend's device of which the battery is dying.

In conventional WPT transmitters (TX), high supply voltage (e.g. >12V) is available [1], which boosts the PA output power, allowing fast charging. However, in our energy-limited battery-to-battery (B2B) scenario, supplying the PA by a Boost converter basically has no benefit due to: 1) additional conversion loss, 2) PA output power level is still constrained by the battery output capability, 3) large area and bulky components required by the Boost, and 4) fast response required by the PA can hardly be satisfied by the Boost. Therefore, to maximize the B2B efficiency and energy transferred, V_{BAT1} supplies the PA directly.

Similarly, V_{BAT2} can be charged directly by the rectifier, eliminating a separate charger [2]. The wide adoption of constant-current mode in wired chargers happens to deliver the maximum rated charging current (usually is the battery-capacity/2-hour for battery health). However, for wireless charging, maximum current rating can hardly be reached, especially in the B2B case. Therefore, it is natural to use the maximum available current for charging, namely the proposed maximum current charging mode (MCCM). Figure 22.4.2 analyzes the WPT charging current I_{CHG} which should not exceed the rated charging current of a typical Li-ion battery. During the charging period, the charging current is found to be an approximately linear function of time where $I_{CHG}=at+b$, with a and b derived from equivalent circuit models. β is a correction factor for imperfect resonance. The calculated and simulated waveforms show that I_{CHG} decreases with time while V_{BAT2} increases. This favors the charging process, because there should be less current at the end of the charging process for less IR drop on the battery internal resistor. Once $V_{OUT}>V_{REF}$ is detected by a hysteresis comparator, the 'End' signal stops the WPT.

Since the power transistors occupy a large silicon area, and the differential Class-D PA and the full-wave active rectifier have very similar symmetrical architectures, Fig. 22.4.3 shows the proposed reconfigurable WPT TRXs that reuses the power transistors and the series resonant tank. For reconfigurations, we use small-size gate-drive multiplexers (MUX_{1-4}) that only deal with signals (not power). In the TX mode, non-overlapping signals control the 4 power transistors, which operate as a differential Class-D PA and drive the LC tank. In the RX mode, we cross-connect M_{P1} and M_{P2}, while M_{N1} and M_{N2} are controlled by the comparators, acting as active diodes [3]. It is noted that $MUX_{1,2}$ should be placed after the gate drive buffer to have the $M_{P1,2}$ being directly driven by the RX AC inputs (not by the buffers), to make the gate capacitors C_g of $M_{P1,2}$ being part of the LC resonant circuit, and thus reducing the switching losses caused by C_g (about 2% RX efficiency improvement in simulation). Hence, we use tri-state buffers with $MUX_{1,2}$. Besides, $MUX_{3,4}$ precede the buffer for smaller MUX size. Another possible solution is to use a single-ended PA for the TX and voltage doubler for the RX, which has the following 4 main drawbacks. 1) To output the same power with the same conduction loss, typical differential and single-ended PAs will occupy the same area, because the differential PA has doubled (+/–) output voltage V_{PA} but also doubled transistor number. However, in this reconfigurable case, one more MUX_7 on the power path is needed for the case shown in Fig. 22.4.3 (bottom). And the MUX_7 needs to conduct the same current as M_P and M_N, which will double the area and conduction loss. 2) Under the same PA supply, the possible solution only attains roughly 1/4 of the I_{CHG} compared to the proposed case, because the voltage doubler would transform the load impedance and the output swing of the single-ended PA is only half of that of the differential PA. 3) The power PMOS in the voltage doubler which needs to be driven by a buffer will cause extra switching loss, when compared with the cross-connected PMOS in the full-wave rectifier case as mentioned above. 4) The voltage doubler needs two additional capacitors C_{L1} and C_{L2} connected in series, which increases the area and cost [4], while the proposed solution could be directly connected to battery.

The proposed reconfigurable WPT TRX is fabricated in a 0.35µm CMOS process with 5V devices, and occupies a chip area of 3.9mm^2. All the results are measured with two identical 4-turn PCB coils (3.3cm of outer diameter) and 6mm WPT distance, at which the measured coupling coefficient k = 0.3. To smooth either the rectifier output current or the PA supply, we use a 1µF capacitor on each side, which is the only off-chip component. Figure 22.4.4 shows the measured steady-state waveforms in both TX and RX modes at P_{OUT}=1.65W, which confirms the effectiveness of the proposed reconfigurable architecture. Figure 22.4.5 shows the measured RX AC input voltages, charging current, and output voltage waveforms, when charging a 1mF capacitor (to emulate the battery). The charging process starts with 1V V_{OUT}, and ends when charged up to 4.2V, which takes <11ms. For the given conditions, the measured maximum charging current is 390mA with an attenuation rate of –5A/s, which basically coincides with the calculated result.

Figure 22.4.6 shows the measured RX and total efficiencies. Due to the elimination of redundant stages in the MCCM, the peak RX and total efficiency reach 91.5% and 58.6%, respectively, at P_{OUT}=1.55W, leading to an observed power loss breakdown of 18%, 23%, and 59% losses from the RX, link, and PA, respectively. The PA efficiency can be improved by a better switching dead-time control. Figure 22.4.6 also gives the comparison with the state-of-the-art. This work achieves the highest level of integration and small chip area with the reconfigurable architecture, and has comparable or higher efficiencies with the MCCM. Figure 22.4.7 shows the chip micrograph and measurement setup.

Acknowledgment:
This work is supported by the Research Committee of the University of Macau under MYRG2015-00107-AMSV, and the Macau Science and Technology Development Fund (FDCT).

References:
[1] H. Park, et al., "A Design of a Wireless Power Receiving Unit With a High-Efficiency 6.78-MHz Active Rectifier Using Shared DLLs for Magnetic-Resonant A4 WP Applications," *IEEE Trans. Power Electron.*, vol. 31, no. 6, pp. 4484–4498, June 2016.
[2] M. Choi, et al., "A Current-Mode Wireless Power Receiver with Optimal Resonant Cycle Tracking for Implantable Systems," *ISSCC*, pp. 372-373, Feb. 2016.
[3] Y. Lu and W.-H. Ki, "A 13.56 MHz CMOS Active Rectifier With Switched-Offset and Compensated Biasing for Biomedical Wireless Power Transfer Systems," *IEEE Trans. Biomed. Circuits Syst.*, vol. 8, no. 3, pp. 334-344, June 2014.
[4] Y. Lu, et al., "A 13.56MHz Fully Integrated 1X/2X Active Rectifier with Compensated Bias Current for Inductively Powered Devices," *ISSCC*, pp. 66-67, Feb. 2013.
[5] J.-H. Choi, et al., "A Resonant Regulating Rectifier (3R) Operating at 6.78 MHz for a 6W Wireless Charger with 86% Efficiency," *ISSCC*, pp. 64-65, Feb. 2013.
[6] M. Kiani, et al., "A Power-Management ASIC with Q-Modulation Capability for Efficient Inductive Power Transmission," *ISSCC*, pp. 226-227, Feb. 2015.
[7] L. Cheng, et al., "A 6.78MHz 6W Wireless Power Receiver with a 3-level 1× / ½× / 0× Reconfigurable Resonant Regulating Rectifier," *ISSCC*, pp. 376-377, Jan. 2016.

 978-1-5090-3758-2/17/$31.00 ©2017 IEEE

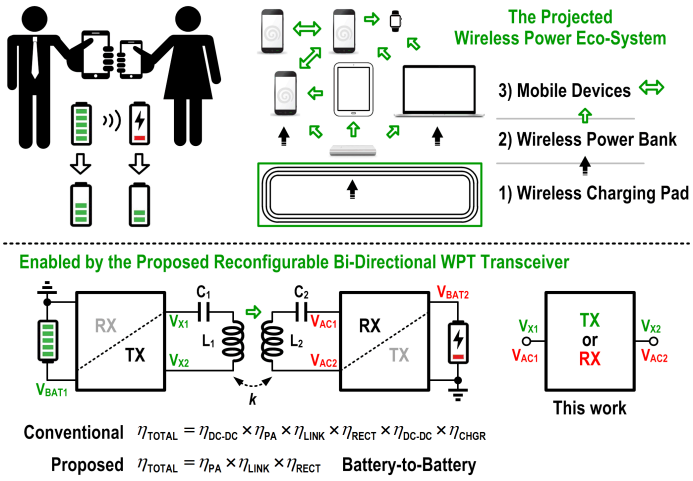

Figure 22.4.1: The projected wireless power eco-system (top) with mobile devices being able to charge each other, enabled by the proposed reconfigurable bi-directional WPT transceiver (bottom).

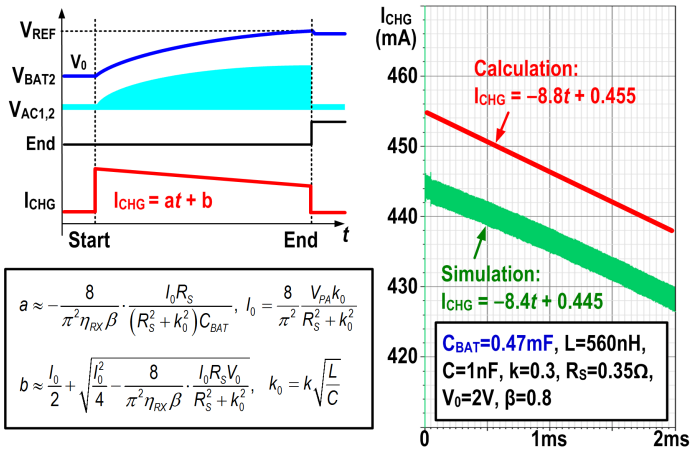

Figure 22.4.2: Proposed maximum-available-current charging scheme with the I_{CHG} equation (left), and the calculated and the transistor-level simulated transient I_{CHG} waveforms (right).

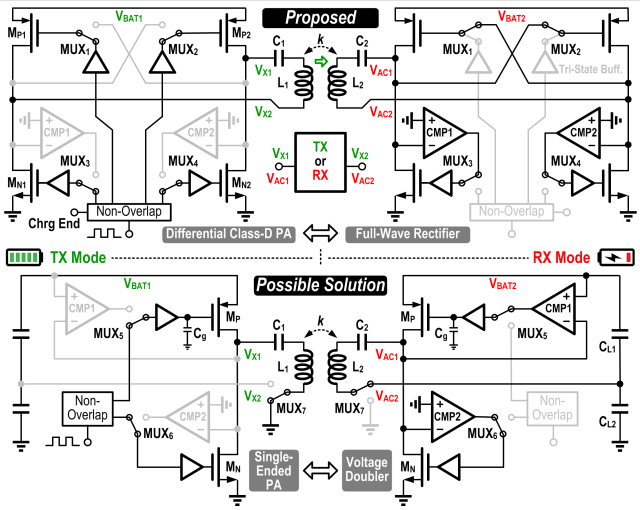

Figure 22.4.3: The proposed reconfigurable bi-directional WPT transceiver (top) that operates as a differential Class-D PA in the TX mode and as a full-wave rectifier in the RX mode, and another possible solution (bottom).

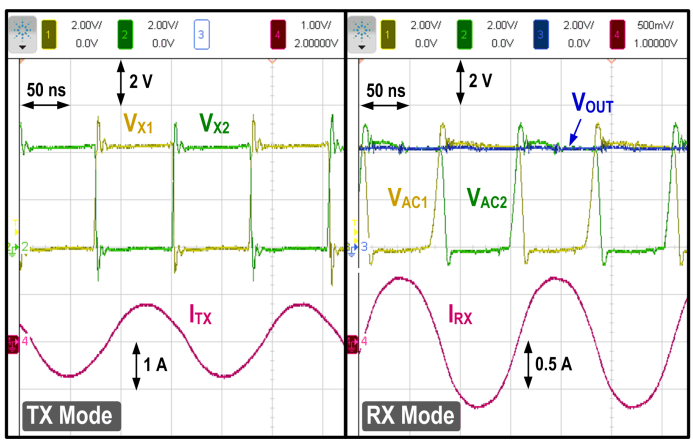

Figure 22.4.4: Measured output voltage/current waveforms in the TX mode, and the input voltage/current and the DC output waveforms in the RX mode, at 1.65W output power.

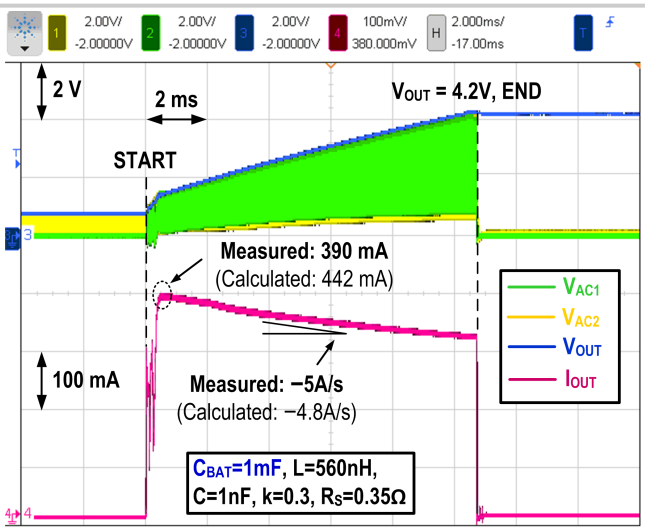

Figure 22.4.5: Measured RX AC input voltage, charging current and output voltage waveforms when charging a 1mF capacitor with MCCM.

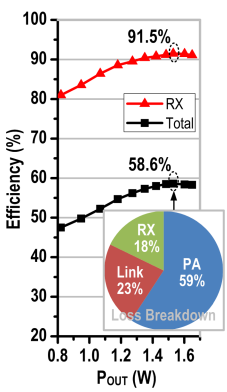

	ISSCC '13 [5]	ISSCC '15 [6]	ISSCC '16 [7]	This Work
Process	0.35μm BCD	0.35μm CMOS	0.35μm CMOS	**0.35μm CMOS**
WPT Direction	Unidirectional	Unidirectional	Unidirectional	**Bi-Directional**
RX Topology	3R	Rectifier+LDO	R^3 Rectifier	**Direct Charge**
$F_{RESONANT}$	6.78MHz	6.78MHz	6.78MHz	**6.78MHz**
Max. V_{OUT}	5V	3V	5V	**4.2V**
Max. P_{OUT}	6W	1.45W	6W	**1.65W**
η_{RX}	86%	75%	92.2%	**91.5%**
η_{TOTAL}	55%	NA	NA	**58.6%**
Area	5.52mm^2 (RX)	4.8mm^2(RX)	4.77mm^2(RX)	**3.9mm^2(TRX)**
Off-Chip Components	5 Diodes, 3 Capacitors	3 Capacitors	1 Capacitor	**1 Capacitor**

Figure 22.4.6: Measured RX and total efficiencies with power loss breakdown, and comparison with the state of the art.

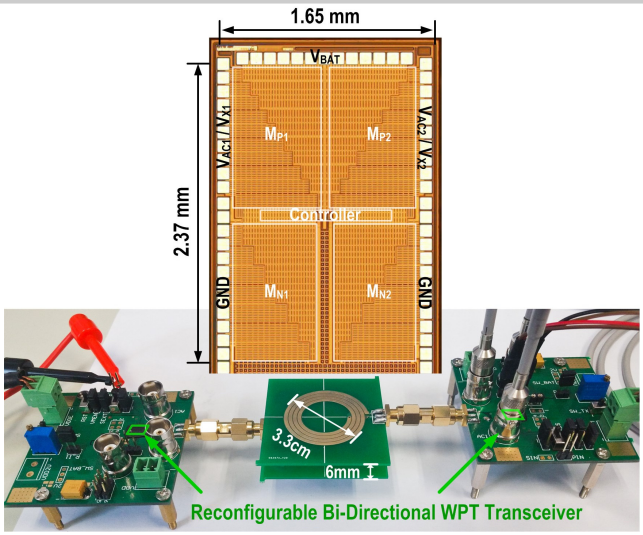

Figure 22.4.7: Die micrograph and measurement setup of the reconfigurable bi-directional WPT TRX.

978-1-5090-3758-2/17/$31.00 ©2017 IEEE